Advanced Concepts for Vertical Stability Power Supply in Fusion Devices

Xiu Yao, *Student Member, IEEE*, Yi Huang, Feng Guo, *Student Member, IEEE*, and Jin Wang, *Member, IEEE*

***Abstract*—Nuclear fusion reactors, such as the tokamak in the International Thermonuclear Experimental Reactor (ITER) project, usually involve extremely sophisticated high-voltage power supply systems, which provide exciting research challenges. In the short term, the major challenges in power supplies of the ITER and other fusion reactors include the following: 1) fast current control of vertical stabilization (VS) coils and 2) dynamic compensation of reactive power and harmonics. In the long term, the power supply systems in fusion reactors provide opportunities for optimizations at both component and system levels. In this paper, modular multilevel converters (M^2LCs) are adopted to tackle the short-term challenges. Circuit structures, pulsewidth-modulation methods, and fault-tolerant operation strategies are presented. The configuration and control strategies of M^2LC in VS coils are fully studied and verified with real-time simulations. Compared with existing circuit solutions in fusion reactors, the M^2LC-based circuits will have better dynamic response, higher reliability, smaller footprint, and reduced weight. As an outlook to the long-term developments of the fusion power supplies, comprehensive real-time simulations are also discussed. Furthermore, as the future development direction of power electronic devices, the wide band gap devices are discussed at the end of this paper.**

***Index Terms*—Control strategy, modular multilevel converter (M^2LC), power supply, real-time simulation, wide band gap devices.**

I. Introduction

NUCLEAR fusion energy is attracting attentions from researchers as an answer to the demand of new energy sources. One of the most promising approaches for nuclear fusion is the tokamak, a reactor based on magnetic confinement [1]. To achieve better performance and desired plasma elongation in tokamaks, vertical stabilization (VS) of the plasma current is required. Traditionally, VS is provided by poloidal field (PF) coils, which are usually placed outside the plasma vessel and require a large amount of currents [2]. However, a delay in control action is induced by the out-of-vessel placement [1]. In addition, the large currents make it not feasible to utilize fast switching devices such as IGBTs and IGCTs. Thus, in-vessel VS coils were proposed to realize fast VS [3]. In-vessel VS coils are located above and under the tokamak's midplate and thus are closer to plasmas. This closeness determines that the current flowing in them cannot be too large [4]. Therefore, while thyristors are the only choice for PF coils due to their high current ratings, it is possible to use fully controllable and faster switching IGBTs and IGCTs in the power supply circuits for VS coils to improve their dynamic responses [5].

In the recent years, different circuit topologies have been studied for the power supply options of VS coils for various nuclear fusion devices all over the world, including the International Thermonuclear Experimental Reactor (ITER) in France, the Experimental Advanced Superconducting Tokamak (EAST) in China, and the Madison Symmetric Torus (MST) in the University of Wisconsin–Madison [6]–[8]. For VS coils in ITER, thyristor-based solution was considered to be more suitable for the continuous operation during two minor events, while the chopper solution with a capacitor bank would be more suitable for the big pulse during the major event due to its minor impact to the grid. A hybrid thyristor and chopper solution was then proposed; however, the disconnection of the chopper after the major event causes challenge to the control [6]. As for EAST, the power is much lower than that of ITER, and the current requirement is different as well. Paralleled diode-clamped multi-inverters with phase-shift pulsewidth modulation (PWM) were proposed to achieve high-power delivery capability and low harmonics [7]. In MST, for the PF coil, a 2700-V and 80-kA power supply system was built based on series–parallel IGBT H-bridge [8]. Among all the aforementioned devices, the power supply for VS coils in ITER is the most challenging one, considering the large current pulse and fast current dynamic response requirements.

Thus, in this paper, the VS coils of the ITER tokamak are used as a case study. The modular multilevel converter (M^2LC) is proposed as the circuit candidate. The main objective is to investigate the control strategies and operation performance of the M^2LC as power supplies of VS coils.

This paper is organized in the following way: Section II provides a general overview of the M^2LC, including its structure, operation principle, and circuit configuration for VS-coil power supplies; Section III proposes the detailed control strategy of M^2LC for VS coils; real-time simulations were conducted, and the results are presented in Section IV; Section V presents the adaptation of the innovative wide band gap devices; and a summary of the work and future plan are shown in Section VI.

II. Operation Principle of M^2LC and Circuit Configuration for VS-Coil Power Supply

A. Operation Principle of M^2LC

The M^2LC was first proposed by Marquardt and Lesnicar in 2002 and then was studied by research teams around the world.

Manuscript received July 29, 2011; revised October 13, 2011; accepted January 4, 2012. Date of publication February 23, 2012; date of current version March 9, 2012.

X. Yao, F. Guo, and J. Wang are with the Department of Electrical and Computer Engineering, The Ohio State University, Columbus, OH 43210 USA.

Y. Huang is with AMETEK, Columbus, OH 43085 USA.

Color versions of one or more of the figures in this paper are available online at http://ieeexplore.ieee.org

Digital Object Identifier 10.1109/TPS.2012.2184550

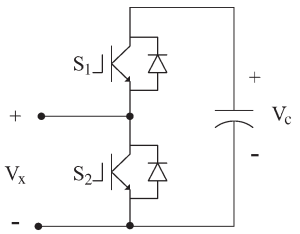

Fig. 1. Structure of a submodule of the M^{2}LC.

TABLE I
SWITCHING STATUS OF A M^{2}LC CELL

Switching status	S_1	S_2	V_x
1	On	Off	V_c
2	Off	On	0

The easy assembling and design flexibility of M^{2}LC circuit makes it suitable for high power conversion. As a member of the multilevel converter family, the introduction of M^{2}LC in power conversion could also eliminate the need for line transformers, as the other multilevel converters do [9]. At present, broad investigations have been carried out for the application in flexible ac transmissions as well as high voltage direct current (HVdc) transmission system. In fact, Siemens has successfully put M^{2}LC in practical use to achieve an almost sinusoidal voltage at the ac output for HVdc transmission systems [10].

The basic cell of the M^{2}LC is a simple half bridge with a capacitor bank, as shown in Fig. 1.

The operation of the two switches in each cell is complementary. The switching status and the output voltage of a cell are shown in Table I. The number of cells in a converter is flexible, which enables convenient voltage and current scaling. Moreover, cells can be uniformly controlled, which greatly eliminates the complexity of the control system and, at the same time, achieves high-quality output voltage and current [11]–[13].

B. Circuit Configuration

Since the current involved in this study is up to 80 kA, no single IGBT is available to handle such a high current level. Thus, paralleling multiple IGBTs in one cell or paralleling multiple cells to form a cell group becomes attractive solutions. However, these paralleling solutions lead to the current sharing problem because of different device parameters and distribution characteristics. Compared with paralleling IGBTs, balancing current among paralleled cells is inherently easier due to the larger distribution inductance which could smooth the circulating current as well as the positive temperature coefficient which is helpful in relaxing the current sharing problem. Because of this, the solution of paralleled cells is applied in this paper. However, it is also worth noting that paralleling IGBT devices has advantages in smaller system size and lower costs although the current imbalance issue is more severe. Recently, the current balancing issue in the parallel connection of IGBTs has been investigated extensively. In [14]–[17], the influence of device parameters and layout to the current imbalance in parallel connection of IGBTs was investigated so that, by consulting with the device manufactures, the device match could be achieved to compensate the imbalance current. Moreover, techniques such as gate circuit control and delay time compensation are also studied for active current balancing [18], [19]. These research results provide a promising future for parallel connection of IGBTs in high-current applications such as the study of this paper.

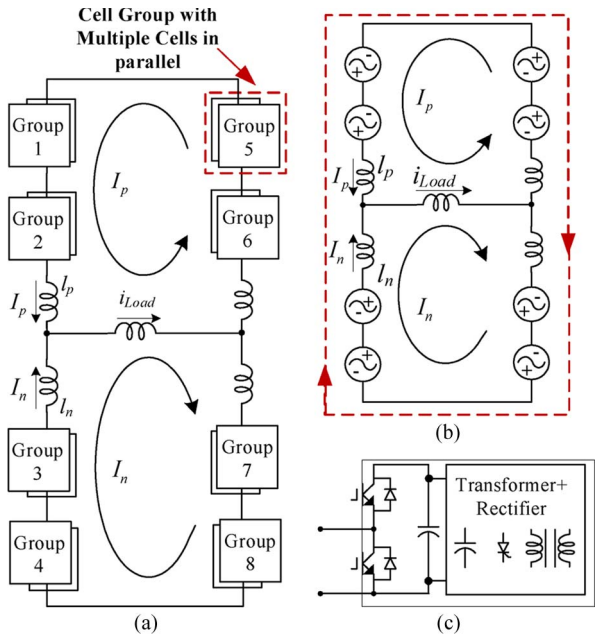

Fig. 2. Circuit configuration of the M^{2}LC. (a) Full circuit structure. (b) Equivalent ac model. (c) Single cell structure.

Fig. 2(a) shows a single-phase M^{2}LC for a VS coil. As mentioned before, multiple cells are paralleled together to form a cell group. Eight cell groups and four buffer inductor cells are used to achieve a five-level load voltage. The cells in each cell group are controlled in the same way. Each cell group can be seen as an ac voltage source with a dc offset.

The equivalent ac model of the overall circuit is shown in Fig. 2(b). The currents go through the buffer inductors ($I_{\rm lp}$ and $I_{\rm ln}$), both equal to half of the load current ($I_{\rm load}$). The buffer inductors' main function is to suppress looping current, and they have little impact on the ac output voltage of the circuit. The looping current is also shown in Fig. 2(b) with a red dashed line.

The direction of the looping current can be different from what is shown depending on the voltage condition of the cell groups. As shown in Fig. 2(c), the dc voltage of each cell in this circuit is supplied by an isolated transformer and a thyristor-based rectifier.

III. CONTROL METHOD OF THE M^{2}LC

A. Current Waveform Requirement for VS Coils

In the preliminary requirements of ITER VS coils, the power supply is required to provide a 0.3-s-long major event of 80-kA pulses every 10 s, two minor events of low-frequency sinusoidal currents at 20 and 10 kA, respectively [6]. Random noise current with an amplitude of less than 3000 A is added on

all the three events. The 80-kA pulse current and transients between each pulse present interesting challenges to the design and control of M^{2}LC. The capacitance and dc voltage source in each group should be designed so as to achieve the required current ramp rate and to provide the large amount of energy during the big pulse.

B. Arm Current Control

The control strategies of M^{2}LC-based circuits have been studied for various applications including HVdc and motor drives. In [12], a combination of averaging and balancing control is proposed to achieve voltage balancing among multiple floating dc capacitors. This control strategy is more suitable for high-power applications such as HVdc. In [13], a control strategy of the M^{2}LC circuit specifically for medium-voltage motor drive application was proposed. Aside from the voltage balancing requirement, the start-up of the motor drive raises more challenges to the circuit control. Thus, the proposed control method in [13] realizes a tradeoff between start-up torque, motor current, and dc voltage fluctuation.

Although the aforementioned existing control strategies can be used as good references, because of the following reasons, a new control strategy still needs to be formed for the proposed M^{2}LC-based VS-coil power supply. First of all, the M^{2}LC circuits in [12] and [13] both utilize a central dc power supply while the M^{2}LC circuit in this paper uses individual dc power supply for each cell group. Moreover, the requirements for VS-coil power supply system are significantly different from that of either HVdc or motor drive applications.

In the proposed control strategy, for the sake of control efficiency and antidisturbance, closed-loop PWM control is applied to control the current flowing through the VS coil. The control strategy has two functions: regulating the load current and eliminating any possible unwanted looping currents. Ideally, the capacitor voltage in all the blocks should be the same; however, this is not the case in real practice. Voltage unbalance always exists due to nonuniform stray inductance of the connections, leakage inductance of the isolation transformers, and different propagation delays in the control circuits of the thyristor-based rectifier. Thus, if the upper branch and lower branch of the circuit are modulated in the same way with unbalanced dc bus voltages, a looping current would be caused by the voltage difference across the buffer inductance, which is shown as the dashed line in Fig. 2(b). The looping current will result in additional switching loss and conducting loss, which could even damage the switching devices. Therefore, an arm control strategy is proposed to solve the looping current problem.

Fig. 3 shows the proposed arm current control strategy. Considering that the load current is the sum of the upper arm current and lower arm current, the main goal of the control strategy is to regulate the arm current I_p and I_n to follow their command $1/2I^*_{\rm ref}$, which is half of the required load current.

In principle, when $I_p < 1/2I^*_{\rm ref}$, cells in groups 5 and 6 will be controlled to output a positive voltage, and cells in groups 1 and 2 will output zero voltage; then, the current will increase and vice versa for the case of $I_p > 1/2I^*_{\rm ref}$.

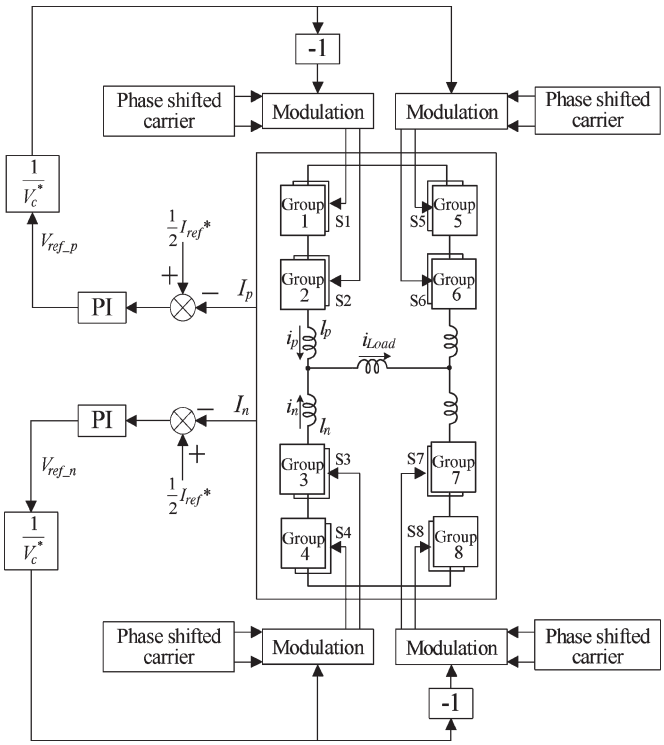

Fig. 3. Control strategy of M^{2}LC.

The two voltage commands for the upper and lower cell groups are obtained with current feedback and PI controllers

$$V_{\rm ref\_p} = K_p\left(\frac{1}{2}I^*_{\rm ref} - I_p\right) + K_i\int\left(\frac{1}{2}I^*_{\rm ref} - I_p\right)dt \quad (1)$$

$$V_{\rm ref\_n} = K_n\left(\frac{1}{2}I^*_{\rm ref} - I_n\right) + K_i\int\left(\frac{1}{2}I^*_{\rm ref} - I_n\right)dt. \quad (2)$$

Then, the voltage commands $V_{\rm ref\_p}$ and $V_{\rm ref\_n}$ are normalized with the capacitor voltage V_c^* before they are used in PWM. Voltage commands $V_{\rm ref\_p}$ and $V_{\rm ref\_n}$ are used to modulate the output voltage of cell groups 5 and 6 $(V_{\rm ru})$ and 3 and 4 $(V_{\rm ll})$, respectively, while $-V_{\rm ref\_p}$ and $-V_{\rm ref\_n}$ are used to modulate cell groups 1 and 2 $(V_{\rm lu})$ and 7 and 8 $(V_{\rm rl})$. To ensure low harmonic distortion and increase the equivalent switching frequency, also shown in Fig. 3, phase-shift multicarrier PWM is adopted for the proposed control strategy. The duty ratio for cell groups 5 and 6 $(V_{\rm ru})$ and cell groups 3 and 4 $(V_{\rm ll})$ can be represented as

$$D_+ = 0.5\left(1 + \frac{V_{\rm ref\_p}}{V_c}\right) \quad (3)$$

$$D_- = 0.5\left(1 - \frac{V_{\rm ref\_p}}{V_c}\right). \quad (4)$$

The equivalent load voltage during one switching cycle is then represented as

$$\begin{aligned}\langle V_{\rm load}\rangle_{\rm Ts} &= D_+ \times 2V_{\rm ru} - D_- \times 2V_{\rm lu}\\ &= 0.5 \times \frac{V_{\rm ref\_p}}{V_c} \times (2V_{\rm ru} + 2V_{\rm lu})\\ &\quad + 0.5 \times (2V_{\rm ru} - 2V_{\rm lu}). \end{aligned} \quad (5)$$

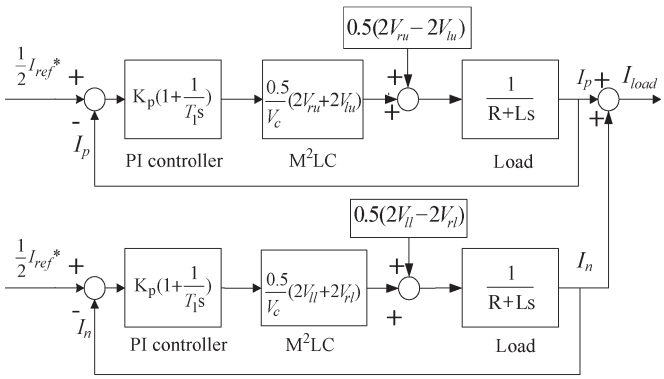

Fig. 4. Block diagram of the M^{2}LC power supply system.

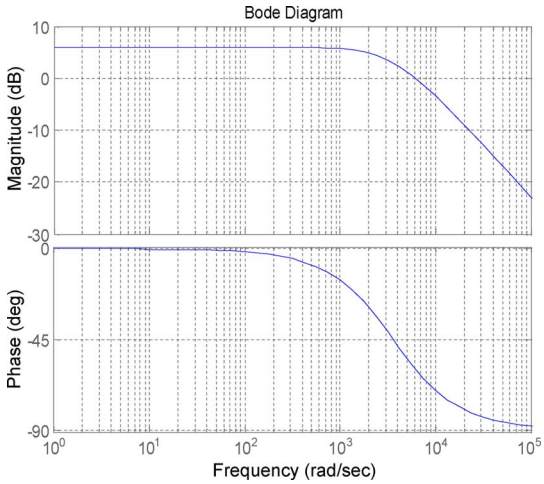

Fig. 5. Block diagram of the M^{2}LC power supply system.

Based on (5), the block diagram of the whole system is shown in Fig. 4.

To simplify the equation, assuming very minor difference between the dc voltages, the closed-loop transfer function can be written as

$$T(s) = 2 \times \frac{K_p s + K_i}{Ls^2 + (R + K_p)s + K_i}. \tag{6}$$

Substituting the variables with preliminary numbers of ITER VS-coil design, the transfer function becomes

$$T(s) = \frac{10s + 20}{1.4 \times 10^{-3} s^2 + 5.01s + 10}. \tag{7}$$

The bode plot of the transfer function is presented in Fig. 5. The phase margin indicates that the system is stable.

IV. Real-Time Simulation

A. Real-Time Simulation Platform

The M^{2}LC-based VS-coil system consists of expensive equipment such as power transformers, rectifiers, and high current switching cells, which make experimental studies of the M^{2}LC economically challenging. Thus, high-fidelity simulations and hardware-in-the-loop-based algorithm verification are often desired.

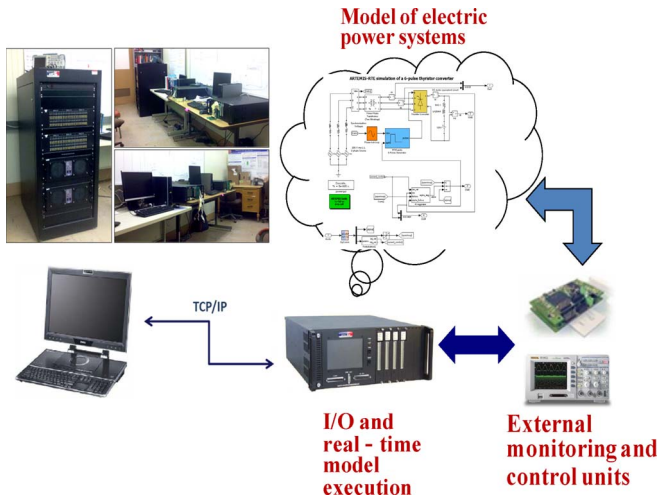

Fig. 6. Real-time simulation for electric power system.

One of the advantages of M^{2}LC power supply is the fast transient property attributed to the implementation of fast switching devices such as IGBTs and IGCTs. However, the high nonlinear switching events and large number of switching devices raise challenges to typical simulation tools, such as pSPICE and Matlab/Simulink. More importantly, offline non-real-time simulation cannot be linked with real devices to realize hardware-in-the-loop functions.

Thus, in this paper, an advanced real-time simulation platform based on PC/field-programmable gate array (FPGA) technology is utilized to verify the proposed control strategies. The hardware platform is composed of four target machines with a total of 6 CPUs, 32 cores, 4 FPGA chips, and more than 500 analog and digital inputs/outputs [1]. Dolphin [21] PCI boards are used to provide an ultrahigh-speed low-latency real-time communication link between target machines. With the technology of switch event interpolation, state-space-nodal solver [22], and parallel computation, the system provides an effective way to realize distributed simulation of multiple subsystems. The switching frequency can be as high as 10 kHz, and a large number of switches can be handled at the same time. The parallel computation capability of this system enables it to run a complex power system model with a maximum of 32 subsystems, and the complete ITER power supply system could be simulated at real time. The real-time simulation platform is shown in Fig. 6. For the work presented in this paper, the M^{2}LC and its controller were simulated with a very light usage of one single CPU.

B. Real-Time Simulation Results With Unbalance Voltage

The parameters of the circuits and controllers are summarized in Table II. In the simulation, 5% unbalance of dc capacitor voltage is introduced to examine the robustness of the proposed control strategy. As mentioned before, the current reference has one major event and two minor events. The possible transients between each event are considered in the current reference. A continuous “noise” at 30 Hz and 3000 A is also added.

TABLE II
CIRCUIT PARAMETERS AND CONTROL GAINS

Load inductance L	1.4 mH
Load resistance R	10 mΩ
Buffer inductance L_p,L_n	5 uH
Module capacitance	2 F
Capacitor voltage in cell groups 1&2 (V_{lu})	1185 V
Capacitor voltage in cell groups 3&4 (V_{ll})	1200 V
Capacitor voltage in cell groups 5&6 (V_{ru})	1230 V
Capacitor voltage in cell groups 7&8 (V_{rl})	1170 V
Carrier frequency	2 kHz
Proportional gain Kp	5 V/A
Integral gain Ki	10V/(A s)

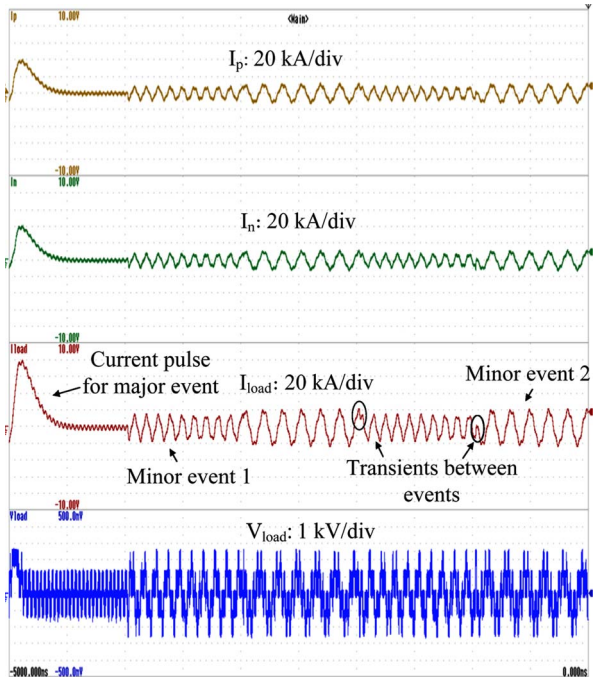

Fig. 7. Real-time simulation results under unbalanced voltage.

Simulation results were observed and recorded via a Yokogawa DL850V digital scope for a total time of 5 s. The simulation results of the two arm currents, the load current, and the output voltage are shown in Fig. 7. These results show that the M^{2}LC, together with the proposed control strategy, could provide pulse current and sinusoidal current that strictly follow the current reference even at the transients between different VS-coil events. The load voltage $V_{\rm load}$ shows a five-level waveform during minor events. The continuous distortion in the voltage waveform is caused by the required "noise" current.

C. Real-Time Simulation Results Under Failure Mode

When a fault occurs to one of the cell groups, that specific cell group could be bypassed by additional switches. The rest of the circuit still could be controlled to follow the control command. Simulations of two cases were carried out to examine the failure tolerance capability of the M^{2}LC circuit.

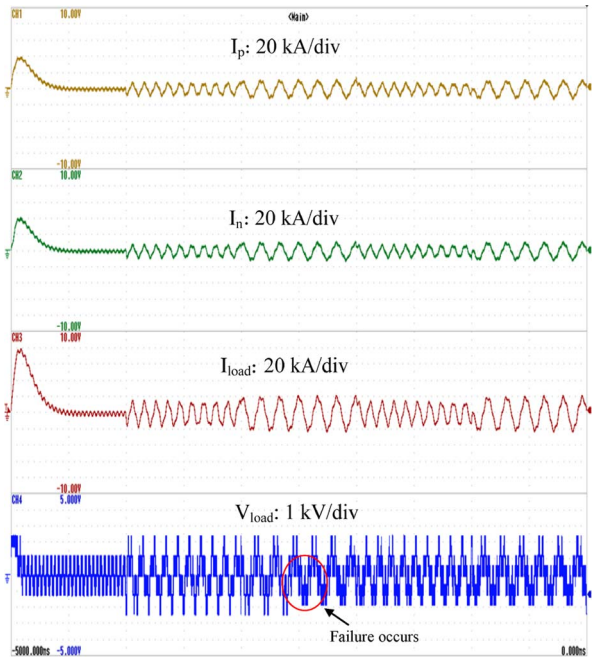

Fig. 8. Real-time simulation results when cell group 1 is failed.

Failure Mode 1—Bypass Group 1: At first, the circuit is operated normally. However, after 2.5 s, a fault occurs, and cell group 1 is intentionally bypassed. The real-time simulation results are shown in Fig. 8. These results show that the proposed control strategy enables the circuit to still operate normally and provide the required current. This is mainly because the remaining dc sources still have enough voltage reserved to derive the desired load current. Because of the same reason, the circuit performance would be the same if one of the cell groups 2, 7, and 8 is bypassed.

Failure Mode 2—Bypass Group 5: A more serious condition would occur when one of the cell groups 3, 4, 5, and 6 fails during the major events. Take cell group 5 for example, after cell group 5 is bypassed at the beginning of a major event, the upper branch of the circuit cannot provide sufficient voltage for the rapid current ramp rate; thus, the required waveform of I_p could not be obtained while I_n still follows the reference. This case is shown in Fig. 9.

To summarize, if one of the cell groups 1, 2, 7, and 8 fails (failure mode 1), the circuit could still operate normally. However, if one of the cell groups 3, 4, 5, and 6 fails (failure mode 2), the system will have impaired performance for the major event.

D. Future Work on Real-Time Simulation

1) Simulation of Reactive Power Compensation With M^{2}LC: Dynamic compensation for reactive power and harmonics is indispensable in the power supply system of a tokamak device considering the large amount of reactive power and harmonics generated by the thyristor-controlled current drives for the magnetic coils. The reactive power will cause fluctuation to the power grid voltage while the harmonics will introduce

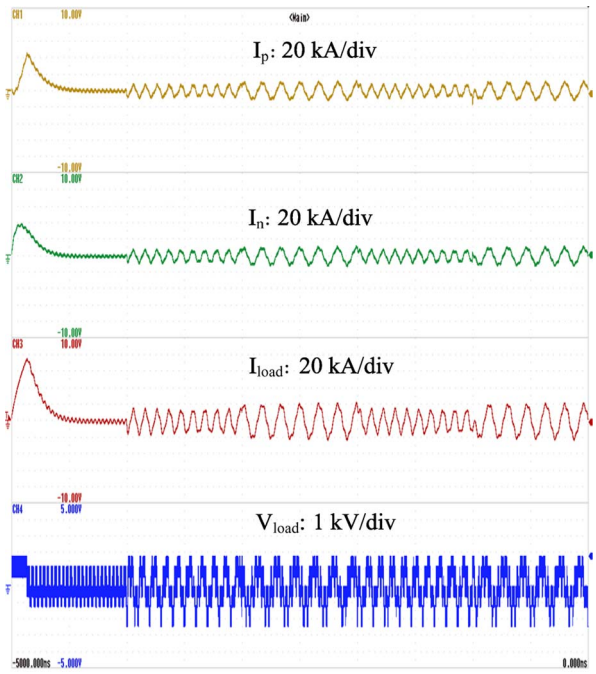

Fig. 9. Real-time simulation results when cell group 5 is failed.

additional heat dissipation and jeopardize the safe operation of the power system and devices. Take ITER for example, the power converter systems will produce up to 840-Mvar reactive power and a high amount of harmonic currents under the 15-MA plasma inductive scenario with a 70-MW heating power [23]. Efforts have been taken to minimize harmonics and reactive power, such as equipping the main step-down transformers with the tertiary windings to allow the circulation of the third harmonic current [24] and realizing sequential control of the converter unit to reduce the reactive power [25]. However, even with the aforementioned methods, the reactive power compensation and harmonic filtering system still has a power rating of 795 Mvar [26].

Considering that the reactive power and harmonic compensation is an indispensable and integral part of the electric power network of a tokamak device, how to utilize the M^2LC to realize dynamic reactive power compensation will be studied and simulated with the real-time simulation platform. Since many papers have been published on the principles of utilizing stand-alone M^2LC in reactive power compensation [27]–[29], therefore, the focus of the study will be the design parameter optimization and control of the hybrid compensation system with both M^2LC-based dynamic compensation and *LC* filter-based passive compensation for tokamaks.

2) Cosimulation of Electric Power and Communication Networks: As mentioned before, the presented real-time simulation platform is capable of simulating the complete power supply network of a tokamak device. Since the tokamak power supply network consists of both electric power systems and communication-based control systems, a combined real-time simulation of electric power network and communication network is proposed as follows: The electric power network will be simulated via the distributed real-time target machines while a system-in-the-loop-based real-time communication network

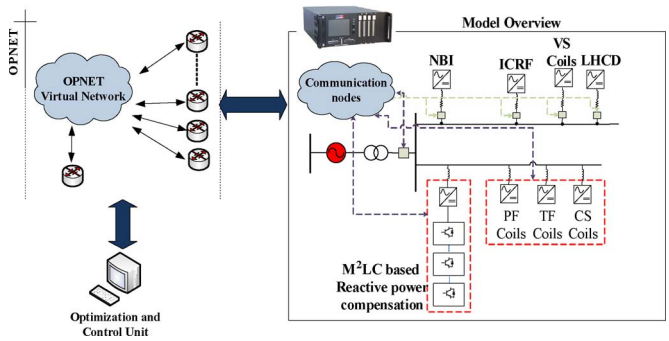

Fig. 10. Real-time simulation of communication network.

simulator will be placed between the simulation model of the electric system and a real digital control unit. This configuration is shown in Fig. 10. With this kind of approach, the hardware-in-the-loop-based simulation for the power supply network is combined with the system-in-the-loop-based simulation of the communication system. Not only the performance of the power supply system can be evaluated at real time but also the impact of communication system imperfection, such as latency and loss of package, could be evaluated.

V. Adaptation of Wide Band Gap Devices

The development of silicon (Si) devices has gradually come to a saturation point due to the limitation on junction temperature of the devices. Future development directions for switching devices include better cooling strategies and wide band gap devices. Compared to Si-based devices, wide band gap devices has major advantages such as higher critical field and higher thermal conductivity, which make them extremely promising for high-power, high-voltage, and high-temperature applications, including the fusion power supply systems. Currently, the most studied wide band gap devices are either based on silicon carbide or gallium nitride.

Silicon carbide (SiC), a wide band gap semiconductor, offers an electric field breakdown voltage ten times that of silicon [30], which makes it possible to develop power electronic switches with higher voltage handling capability. This higher voltage capability reduces the number of switches required and thus reduces the problem of voltage balance among different switches. The thermal conductivity of SiC is also much higher than that of Si, 3.7 $W/cm \cdot K$ for the former compared to 1.3 $W/cm \cdot K$ for the latter [30]. Along with the higher junction temperature (normally 300 °C), the SiC devices show a significant improvement in power dissipation [31]. The higher junction temperature also relaxes the requirement of the cooling system for SiC switches, and thus, the size of the cooling system could be reduced. Therefore, the SiC-based devices have obvious volume advantages compared to Si-based devices with comparable voltage ratings. This forms a major advantage considering the limited free space around ITER system.

Nowadays, SiC Schottky rectifier products are available from CREE, Inc., SiCED, Semisouth Laboratories, etc. [32]–[34]. Other SiC devices that have been developed include MOSFETs, SiC GTOs and thyristors, and SiC IGBTs in the 10-kV class. SiC MOSFETs are the most mature and are more suitable for

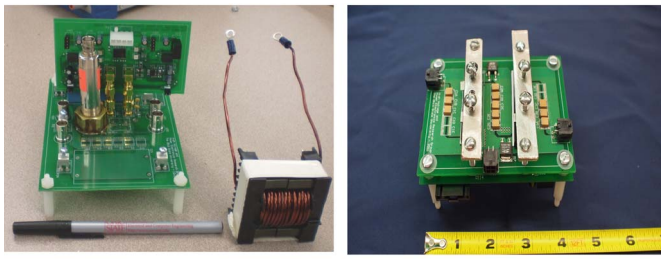

(a) (b)

Fig. 11. GaN test boards. (a) GaN test platform. (b) GaN HEMT prototype.

high-frequency applications due to the low switching losses [35]. Modules with 1200-V and 100-A rating have been demonstrated. The application of SiC devices has been under extensive investigation among universities and research organizations. For example, the utilization of SiC devices in hybrid vehicles has been investigated in [36], showing the capability of a SiC DMOSFET in situations where the performance of Si devices is limited by switching losses and junction temperature. In addition, the application of SiC super gate turnoff thyristors in pulsed power applications has been investigated by the Army Research Laboratory [37].

Gallium nitride (GaN) is another type of wide band gap semiconductor with promising characteristics in critical electric field, temperature, and switching speed [38]–[41]. So far, GaN is not as well developed as SiC devices. Nevertheless, GaN test platforms and demonstration circuits are reported from both universities and industrial laboratories. A multifunctional GaN test board is shown in Fig. 11(a). A 600-W GaN-based switched capacitor prototype is shown in Fig. 11(b). These circuits demonstrated the high switching speed, low conduction loss, and third quadrant operation of GaN high electron mobility transistors (HEMTs) [42].

Although there is still a long way for GaN devices to be utilized in fusion power supplies, the fusion research is also an ongoing effort. The next international demonstration project is still years away. Therefore, it is a good time to investigate the new technologies for future fusion applications.

VI. Conclusion

In this paper, three advanced concepts for power supplies of nuclear fusion reactors have been introduced. First, the study of utilizing the M^2LCs for VS coils, with a focus on its control method and operation performance, is presented. Arm current control strategy is proposed to eliminate the looping current caused by the voltage unbalance among different modules. Then, an advanced real-time simulation platform is introduced as an effective tool for control strategy validations. In particular, the real-time simulation results of a M^2LC-based VS-coil power supply are shown to verify the proposed control scheme. Failure tolerance of the proposed system is also investigated. Results show that the circuit operation under failure mode can be different depending on which specific cell group fails. At the end, the development of wide band gap power devices and the potential of utilizing them in the fusion power system are briefly discussed.

References

[1] G. Ambrosino, M. Ariola, G. De Tommasi, and A. Pironti, "Plasma vertical stabilization in the ITER tokamak via constrained static output feedback," *IEEE Trans. Control Syst. Technol.*, vol. 19, no. 2, pp. 376–381, Mar. 2001.

[2] M. Ariola, G. Ambrosino, and A. Pironti, "Design and experimental testing of a robust multivariable controller on a tokamak," *IEEE Trans. Control Syst. Technol.*, vol. 10, no. 5, pp. 646–653, Sep. 2002.

[3] P. J. Heitzenroeder, A. W. Brooks, J. H. Chrzanowski, F. Dahlgren, R. J. Hawryluk, G. D. Loesser, C. Neumeyer, C. Mansfield, J. J. Cordier, D. Campbell, G. A. Johnson, A. Martin, P. H. Rebut, J. O. Tao, J. P. Smith, M. Schaffer, D. Humphreys, P. J. Fogarty, B. E. Nelson, and R. P. Reed, "An overview of the ITER in-vessel coil systems," in *Proc. 23rd IEEE/NPSS Symp. Fusion Eng.*, San Diego, CA, 2009, pp. 1–4.

[4] P. Heitzenroeder, System Requirements Document for the In-Vessel Coils, Dec. 2008, ITER IDM No. ITER_D_2MFYMWv1.0.

[5] M. Toyoda, Y. Kikuchi, Y. Uesugi, and S. Takamura, "Fast feedback control of plasma horizontal position by using DSP and IGBT inverter," *Elect. Eng. Japan*, vol. 148, no. 1, pp. 1–10, Jul. 2004.

[6] "Development of power supply concept for in-vessel coil," in *Proc. STAC 5th ITER Meeting*, Cadarcahe, France, Oct. 2008, pp. 20–22.

[7] P. Fu, Z. Liu, G. Gao, L. Yang, Z. Q. Song, L. W. Xu, J. Tao, and X. N. Liu, "Power supply system of EAST superconducting tokamak," in *Proc. IEEE 5th Conf. Ind. Elect. Appl.*, Taichung, Taiwan, 2010, pp. 457–462.

[8] R. Albanese, G. Ambrosino, M. Ariola, M. Cavinato, G. De Tommasi, Y. Liu, M. Mattei, A. Pironti, A. Portone, G. Rubinacci, G. Saibene, F. Sartori, and F. Villone, "ITER vertical stabilization system," *Fusion Eng. Des.*, vol. 84, no. 2–6, pp. 394–397, Jun. 2009.

[9] J. Rodriguez, J. S. Lai, and F. Z. Peng, "Multilevel inverters: A survey of topologies, controls, and applications," *IEEE Trans. Ind. Electron.*, vol. 49, no. 4, pp. 724–738, Aug. 2002.

[10] Seimens, Inc. [Online]. Available: http://www.siemens.com/entry/cc/en/

[11] R. Marquardt and A. Lesnicar, "A new modular voltage source inverter topology," presented at the Conf. Rec. EPE, Toulouse, France, 2003, [CD-ROM].

[12] M. Hagiwara and H. Akagi, "Control and experiment of pulsewidth-modulated modular multilevel converters," *IEEE Trans. Power Electron.*, vol. 24, no. 7, pp. 1737–1746, Jul. 2009.

[13] M. Hagiwara, K. Nishimura, and H. Akagi, "A medium-voltage motor drive with a modular multilevel PWM inverter," *IEEE Trans. Power Electron.*, vol. 25, no. 7, pp. 1737–1746, Jul. 2010.

[14] H. Yang, W. Xuhui, G. Lingyun, W. Li, and Z. Feng, "Investigation of parallel connection of IGBTs," in *Proc. 8th Int. Conf. Elect. Machines Syst.*, Sep. 2005, vol. 1, pp. 833–835.

[15] J. Nelson, G. Venkataramanan, and B. C. Beihoff, "Investigation of parallel operation of IGBTs," in *Conf. Rec. 37th IEEE IAS Annu. Meeting*, 2002, pp. 2585–2591.

[16] H. Miyazaki, H. Fukumoto, S. Sugiyama, M. Tachikawa, and N. Azusawa, "Neutral-point-clamped inverter with parallel driving of IGBT's Industrial Applications," *IEEE Trans. Ind. Appl.*, vol. 36, no. 1, pp. 146–151, Jan./Feb. 2000.

[17] F. Chimento, F. Nicosia, S. Musumeci, A. Raciti, M. Melito, and G. Sorrcntino, "Simulation and behavior evaluation of PT-IGBT connections in parallel strings," in *Proc. IEEE Int. Symp. Ind. Elect.*, Vigo, Spain, Jun. 2007, pp. 931–936.

[18] D. Bortis, J. Biela, and J. W. Kolar, "Active gate control for current balancing of parallel-connected IGBT modules in solid-state modules," *IEEE Trans. Plasma Sci.*, vol. 36, no. 5, pp. 2632–2637, Oct. 2008.

[19] R. Alvarez and S. Bernet, "A new delay time compensation principle for parallel connected IGBTs," in *Proc. IEEE 3rd Annu. Energy Convers. Congr. Expo.*, Phoenix, AZ, Jul. 2011, pp. 3000–3007.

[20] Opal-RT Technologies. [Online]. Available: http://www.opalrt.com

[21] Dolphin. [Online]. Available: http://www.dolphinics.com

[22] C. Dufour, J. Mahseredjian, and J. Belanger, "A combined state-space nodal method for the simulation of power system transients," *IEEE Trans. Power Del.*, vol. 26, no. 2, pp. 928–935, Apr. 2011.

[23] L. Xu, Z. Sheng, P. Fu, G. Gao, A. D. Benfatto Mankani, and J. Tao, "The reactive power compensation and harmonic filtering and the overvoltage analysis of the ITER power supply system," in *Proc. IEEE 25th Annu. Appl. Power Elect. Conf. Expo.*, Palm Springs, CA, Feb. 2010, pp. 1622–1626.

[24] A. Roshal, B. Bareyt, I. Benfatto, N. Britousov, D. Hrabal, K. Krueger, A. Maschio, P. L. Mondino, and T. Shoji, "The ITER-FEAT power supply system and interface with the site HV power grid," *Fusion Eng. Des.*, vol. 58/59, pp. 87–91, Nov. 2001.

[25] P. Fu, G. Gao, L. W. Xu, Z. Q. Song, Z. C. Sheng, J. S. Oh, I. Benfatto, J. Tao, A. D. Mankani, and C. Neumeyer, "Review and analysis of the ac/dc converter of ITER coil power supply," in *Proc. 25th Annu. IEEE Appl. Power Electron. Conf. Expo.*, 2010, pp. 1810–1816.
[26] L. Xu, Z. Sheng, and P. Fu, "The reactive power compensation and harmonic filtering and the over-voltage analysis of the ITER power supply system," in *Proc. 25th Annu. IEEE Appl. Power Electron. Conf. Expo.*, 2010, pp. 1622–1626.
[27] M. Hagiwara, R. Maeda, and H. Akagi, "Negative-sequence reactive-power control by the modular multilevel cascade based on double-star chopper cells (mMCC-dSCC)," in *Proc. IEEE ECCE*, 2010, pp. 3949–3954.
[28] H. Akagi, "Classification, terminology, and application of modular multilevel cascade converter," *IEEE Trans. Power Electron.*, vol. 26, no. 11, pp. 3119–3130, Nov. 2011.
[29] H. P. Mohammadi and M. T. Bina, "A transformerless medium-voltage STATCOM topology based on extended modular multilevel converters," *IEEE Trans. Power Electron.*, vol. 26, no. 5, pp. 1534–1545, May 2011.
[30] J. Richmond, S. Leslie, B. Hull, M. Das, A. Agarwal, and J. Palmour, "Roadmap for megawatt class power switch modules utilizing large area silicon carbide MOSFETs and JBS diodes," in *Proc. Energy Convers. Congr. Expo.*, 2009, pp. 106–111.
[31] T. E. Salem, D. P. Urciuoli, R. Green, and G. K. Ovrebo, "High-temperature high-power operation of 100 A SiC DMOSFET module," in *Proc. 24th IEEE Appl. Power Electron. Conf. Expo.*, 2009, pp. 653–657.
[32] CREE, Inc. [Online]. Available: http://www.cree.com/products
[33] SiCED. [Online]. Available: http://www.siced.de
[34] Semisouth. [Online]. Available: http://www.semisouth.com
[35] Q. J. Zhang, R. Callamanm, M. K. Das, S.-H. Ryu, A. K. Agarwal, and J. W. Palmour, "SiC power devices for microgrids," *IEEE Trans. Power Electron.*, vol. 25, no. 12, pp. 2889–2896, Dec. 2010.
[36] R. Kelly, M. S. Mazzola, and V. Bondarenko, "A scalable SiC device for dc/dc converter future hybrid electric vehicles," in *Proc. 21st IEEE Appl. Power Electron. Conf. Expo.*, 2006, pp. 460–464.
[37] A. Ogunniyi, H. O'Brien, A. Lelis, C. Scozzie, W. Shaheen, A. Agarwal, J. Zhang, R. Callanan, and V. Temple, "The benefits and current progress of SiC SGTOs for pulsed power applications," *Solid State Electron.*, vol. 54, no. 10, pp. 1232–1237, Oct. 2010.
[38] J. W. Milligan, S. Sheppard, W. Pribble, A. Ward, and S. Wood, "SiC and GaN wide bandgap technology commercial status," in *Proc. CS MANTECH Conf.*, Chicago, Illinois, Apr. 14–17, 2008, pp. 1–4.
[39] W. Saito, T. Nitta, Y. Kakiuchi, Y. Saito, K. Tsuda, I. Omura, and M. Yamaguchi, "A 120-W boost converter operation using a high-voltage GaN-HEMT," *IEEE Electron Device Lett.*, vol. 29, no. 1, pp. 8–10, Jan. 2008.
[40] D. Ueda, M. Hikita, S. Nakazawa, K. Nakazawa, H. Ishida, M. Yanagihara, K. Inoue, T. Ueda, Y. Uemoto, T. Tanaka, and T. Egawa, "Present and future prospects of GaN power electronics," in *Proc. 9th Int. Conf. Solid-State Integr.-Circuit Technol.2008*, pp. 1078–1081.
[41] M. A. Kahn, G. Simin, S. G. Pytel, A. Monti, E. Santi, and J. L. Hudgins, "New developments in gallium nitride and the impact on power electronics," in *Proc. IEEE 36th Power Electron. Spec. Conf.*, 2005, pp. 15–26.
[42] M. J. Scott, K. Zou, and J. Wang, "A gallium-nitride switched-capacitor circuit using synchronous rectification," in *Proc. 3rd Annu. IEEE Energy Convers. Congr. Expo.*, Jul. 2011, pp. 2501–2505.

Xiu Yao (S'10) received the B.S. and M.S. degrees from Xi'an Jiaotong University, Xi'an, China, in 2007 and 2010, respectively. She is currently working toward the Ph.D. degree at The Ohio State University, Columbus.

Her current research interests include the utilization of modular multilevel converter in fusion engineering, harmonic elimination of multilevel inverter, and dc arc fault detection in high voltage and power electronic systems.

Yi Huang received the B.S. and M.S. degrees in electrical engineering from the Wuhan University, Wuhan, China, in 1998 and 2001, respectively, and the Ph.D. degree in electrical engineering from the Michigan State University, East Lansing, in 2009.

From December 2009 to May 2011, she was with The Ohio State University, Columbus, as a Postdoctoral Researcher. She is currently with AMETEK, Columbus, OH. Her research areas include dc–ac inverter, dc–dc converter, advanced digital control technique, and photovoltaic inverter systems.

Feng Guo (S'09) was born in Henan, China, in 1986. He received the B.S. degree in electrical engineering from Wuhan University, Wuhan, China, in 2009. He is currently working toward the Ph.D. degree at The Ohio State University, Columbus.

His current research interests include large-scale PV power plant with local energy storage, hardware-in-the-loop and real-time simulation of smart grid, power electronics circuits in hybrid electric vehicles, and energy harvesting around high-voltage transmission line.

Jin Wang (S'02–M'05) received the B.S. degree in electrical engineering from Xi'an Jiaotong University, Xi'an, China, in 1998, the M.S. degree in electrical engineering from Wuhan University, Wuhan, China, in 2001, and the Ph.D. degree in electrical engineering from Michigan State University, East Lansing, in 2005.

From September 2005 to August 2007, he was with the Ford Motor Company as a Core Power Electronics Engineer and contributed to the traction drive design of the Ford Fusion Hybrid. Since September 2007, he has been an Assistant Professor with the Department of Electrical and Computer Engineering, The Ohio State University, Columbus. His teaching position is cosponsored by American Electric Power, Duke/Synergy, and FirstEnergy. His research interests include high-voltage and high-power converter/inverters, integration of renewable energy sources, and electrification of transportation.

Dr. Wang was the recipient of the IEEE Power Electronics Society Richard M. Bass Young Engineer Award and the National Science Foundation's CAREER Award, both in 2011. He has over 50 peer-reviewed journal and conference publications. He has been an Associate Editor for IEEE TRANSACTIONS ON INDUSTRY APPLICATION since March 2008.